



RESEARCH ARTICLE | MAY 27 2022

Polaritonic effects in the vibronic spectrum of molecules in an optical cavity

Marta L. Vidal ; Frederick R. Manby ; Peter J. Knowles 



J. Chem. Phys. 156, 204119 (2022)

<https://doi.org/10.1063/5.0089412>



APL Quantum

First Articles Online

No Article Processing Charges for Submissions
Through December 31, 2024

[Read Now](#)

Polaritonic effects in the vibronic spectrum of molecules in an optical cavity

Cite as: J. Chem. Phys. 156, 204119 (2022); doi: 10.1063/5.0089412

Submitted: 25 February 2022 • Accepted: 28 April 2022 •

Published Online: 27 May 2022



View Online



Export Citation



CrossMark

Marta L. Vidal,^{1,a)} Frederick R. Manby,² and Peter J. Knowles¹

AFFILIATIONS

¹School of Chemistry, Cardiff University, Main Building, Park Place, Cardiff CF10 3AT, United Kingdom

²School of Chemistry, University of Bristol, Cantocks Close, Bristol BS8 1TS, United Kingdom

^{a)}Author to whom correspondence should be addressed: mrtlvd@gmail.com and knowlespj@cardiff.ac.uk

ABSTRACT

We present a new computational framework to describe polaritons, which treats photons and electrons on the same footing using coupled-cluster theory. As a proof of concept, we study the coupling between the first electronically excited state of carbon monoxide and an optical cavity. In particular, we focus on how the interaction with the photonic mode changes the vibrational spectroscopic signature of the electronic state and how this is affected when tuning the cavity frequency and the light–matter coupling strength. For this purpose, we consider different methodologies and investigate the validity of the Born–Oppenheimer approximation in such situations.

© 2022 Author(s). All article content, except where otherwise noted, is licensed under a Creative Commons Attribution (CC BY) license (<http://creativecommons.org/licenses/by/4.0/>). <https://doi.org/10.1063/5.0089412>

I. INTRODUCTION

Polariton chemistry, which studies the strong interaction between photons and molecules, has been subject to increasing interest in recent years. The origin of this growing attention lies in the fact that when light strongly interacts with matter, it can modify its physical and chemical properties. Whereas physicists have long studied this phenomenon¹ principally due to its promising potential in a variety of areas, ranging from light amplification^{2,3} to quantum computing,^{4,5} it is only in the last decade that the chemistry community has started focusing on polaritonic effects.⁶ Even though the existence of hybridized light–matter states in inorganic materials had also been known for some time, it was only at the end of the last century that it was shown that this strong coupling effect could be enhanced by optical cavities.⁷ This discovery was crucial to the development of polaritonic chemistry; however, more recent and abundant interest in the field comes from the realization that by tuning the coupling between light and a chemical system, one might be able to modify its properties and even control chemical reactions⁸ by, for instance, modifying intersystem crossings and conical intersections.^{9,10} Examples include the modification of photoisomerization yields¹¹ and of the rate of organic reactions,^{12–14} boosting of conductivity,¹⁵ and enhancement of the optical activity of a material.¹⁶ For a more complete list, please see the recent reviews of Refs. 7 and 17.

When the strength of the coupling between photonic and electronic degrees of freedom becomes significant on the scale of Coulombic interactions in the molecule, it results in the hybridization between the two states. As already anticipated, these new hybrid light–matter states can be formed by placing the quantum system in an optical cavity, which consists of two parallel mirrors, as represented in Fig. 1. By tuning the cavity frequency ω_c such that it approaches resonance with excitation energy of the molecule, the photonic state and the electronic state will give rise to two hybrid light–matter states—an upper (UP, $|p^+\rangle$) polariton and a lower (LP, $|p^-\rangle$) polariton—separated in energy by the Rabi splitting. This is illustrated in Fig. 2, where one can see how the states of a system are altered inside a quantum optical cavity.

The quantum mechanical treatment of the polaritonic system needs to embrace the entire molecule–cavity system, rather than treating it as an electronic system in the presence of an external classical electromagnetic field. A number of attempts have been made to extend electronic theories to the polaritonic domain, by including quantum electrodynamical effects. Among them, the first was QEDFT, which introduces QED effects into density functional theory (DFT),^{18–20} being the most widespread electronic structure method due to its relative computational cost with wavefunction theories. More recently, QED effects have been introduced into coupled-cluster (CC) theory, which offers an opportunity to recover most of the electronic correlation at a reasonable computational

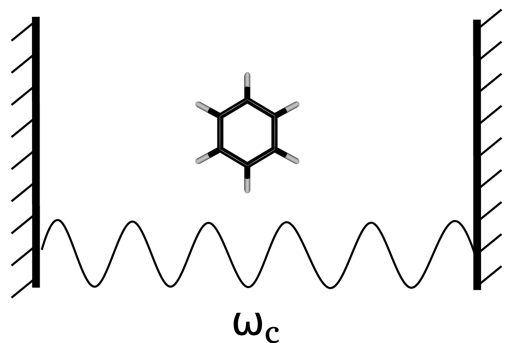


FIG. 1. Schematic representation of a molecule in an optical cavity.

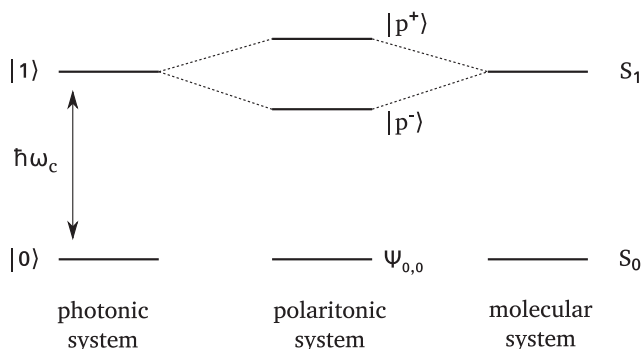


FIG. 2. Schematic representation of the hybridization between light and matter states.

cost, scaling polynomially with the size of the system. CC theory was first developed for nuclear^{21,22} structure and electronic^{23–25} problems, and has enjoyed widespread use and success for molecular electronic structure. It has also been applied to nuclear motion^{26,27} and, more recently, to polaritons.^{28–31} We present here the extension of the CC framework of Ref. 28 that treats electrons and photons on an equal footing, and, in particular, of its excited-state method equation-of-motion coupled cluster (EOM-CC) for the full quantum chemical Hamiltonian.

II. THEORY

A. Hamiltonian

We take the following Hamiltonian operator in the length (L) gauge for an isolated molecule inside a cavity with one or more optical modes:³²

$$\hat{\mathcal{H}}_L = \hat{\mathcal{H}}_e + \hat{T}_n + \sum_{\kappa} \left[\hbar\omega_{\kappa} \left(b^{\dagger} b + \frac{1}{2} \right) - \sqrt{\hbar} \omega_{\kappa} (\mathbf{y}_{\kappa} \cdot \boldsymbol{\mu}) (\hat{b} + \hat{b}^{\dagger}) + \omega_{\kappa} (\mathbf{y}_{\kappa} \cdot \boldsymbol{\mu})^2 \right]. \quad (1)$$

Here, $\hat{\mathcal{H}}_e$ is the usual field-free clamped-nucleus electronic Hamiltonian, \hat{T}_n is the nuclear kinetic energy (NKE) operator, and $\boldsymbol{\mu}$ is the dipole operator (for both nuclei and electrons). The last two terms

introduce the interaction between the particles and the photon field, with κ labeling a cavity mode with harmonic-oscillator stationary states of characteristic angular frequency ω_{κ} . The penultimate term in the Hamiltonian is linear in both particle and cavity coordinates, and causes correlation between cavity and molecule states. Finally, the last term is the self-energy of the molecule in the radiation field, and is positive definite. The coupling enters the Hamiltonian via the coupling parameter,

$$\boldsymbol{y}_{\kappa} = \frac{\boldsymbol{\lambda}_{\kappa}}{\sqrt{2\omega_{\kappa}}} = \frac{1}{\sqrt{2\omega_{\kappa}}} \sqrt{\frac{1}{\epsilon_0 V}} \boldsymbol{\epsilon}_{\kappa}, \quad (2)$$

where $\boldsymbol{\epsilon}_{\kappa}$ is a unit vector in the electric polarization direction of the cavity mode and V is the cavity volume.

In all of the calculations considered here, we take a single cavity mode, and ignore the effects of molecular rotation and translation, explicitly orienting the molecule relative to $\boldsymbol{\epsilon}_{\kappa}$, but including in \hat{T}_n the motion of the nuclei along the vibrational normal coordinates.

B. EOM-CC for electrons and bosons

In equation-of-motion (EOM) coupled-cluster (CC) theory for fermions,³² the ground state is described at the CC level, with a wavefunction given by the following exponential ansatz:

$$|\Psi_{\text{CC}}\rangle = e^{\hat{\mathcal{T}}} |\Phi_0\rangle, \quad \hat{\mathcal{T}} = \sum_{\mu} \hat{\tau}_{\mu}, \quad (3)$$

where $|\Phi_0\rangle$ is the reference state, typically taken as the Hartree–Fock (HF) Slater determinant ($|\Phi_{\text{HF}}\rangle$), and $\hat{\mathcal{T}}$ is known as the cluster operator. Here, the subscript μ refers to the level of excitation, not to be confused with the dipole moment operator, and $\hat{\tau}_{\mu}$ is a linear combination of a product of μ annihilation and μ creation operators,

$$\hat{\tau}_{\mu} = (\mu!)^{-2} t_{ab\dots}^{ij\dots} \hat{a}_a^{\dagger} \hat{a}_b^{\dagger} \dots \hat{a}_j \hat{a}_i, \quad (4)$$

having the effect of making μ -fold excitations from HF-occupied one-particle states, and serves to construct a correlated wavefunction.

The energy and the cluster amplitudes are determined by the CC equations,

$$\langle \Phi_0 | \hat{\mathcal{H}} | \Phi_0 \rangle = E_{\text{CC}}, \quad (5)$$

$$\langle \Phi_0 | \hat{a}_i^{\dagger} \hat{a}_j^{\dagger} \dots \hat{a}_b \hat{a}_a \hat{\mathcal{H}} | \Phi_0 \rangle = 0, \quad (6)$$

where the similarity-transformed Hamiltonian $\hat{\mathcal{H}} \equiv e^{-\hat{\mathcal{T}}} \hat{\mathcal{H}} e^{\hat{\mathcal{T}}}$ has been introduced.

The excited states are then accessed by the linear parameterization,³²

$$|\Psi_n\rangle = \hat{\mathcal{R}}_n |\Phi_{\text{CC}}\rangle, \quad (7)$$

where the excitation operator $\hat{\mathcal{R}}$ has the same form as the cluster operator but with different amplitudes $r_{ab\dots}^{ij\dots}$. Thus, the excited states are obtained as eigensolutions of the similarity-transformed Hamiltonian matrix, as follows:

$$\hat{\mathcal{H}} \mathcal{R}_n = \mathcal{R}_n E_n. \quad (8)$$

The similarity-transformed Hamiltonian is not Hermitian, and so the left eigenvectors \mathcal{L}_n are different to \mathcal{R}_n , and both are needed for calculating the properties that depend on the wavefunction in an exact treatment.³² However, if one is interested only in the excitation energies, it is sufficient to solve just the right eigenproblem.

Even though EOM-CC was originally conceived for the electronic problem, there are no *a priori* reasons to restrict its use to the treatment of electrons only. However, the standard CC formalism is usually expressed explicitly in terms of the field operators for electrons, embedding their fermionic nature, and the single electron spin doublet. However, it is possible to use this formalism almost unchanged, by a pseudo-particle treatment of bosonic modes of motion, and a generalization of the spin-symmetry separation used in the conventional electronic structure theory.

To extend the EOM-CC method to the treatment of bosonic systems, we adopt the formalism first presented in Ref. 28, which follows an earlier work by Christiansen.²⁶ In this framework, the number of bosons is restricted to n_{\max} such that a given bosonic mode can be mapped to a basis of $n_{\max} + 1$ states, each representing a different number of bosons in the same state, which can be written as $|0\rangle, |1\rangle, \dots, |n_{\max}\rangle$. To each number state, one can then associate an excitation operator $\hat{\tau}_n = |n\rangle\langle 0|$ that creates that state from the vacuum. The bosonic quantum mechanics can then be expressed entirely in terms of a Hilbert space for a fictitious single particle whose stationary states represent the boson number states. Because there is just one pseudo-particle, it does not matter whether it is treated as a fermion or a boson, and in a second-quantized treatment, the Fermi level is directly above $|0\rangle$; $|n\rangle\langle 0|$ is then equivalent to annihilation of the ground-state pseudo-particle, followed by creation of it in an excited state.

In the case of more than one type of boson (cavity modes or vibrational normal modes), each mode will have its own non-identical pseudo-particle. We can then choose to treat the pseudo-particle as a fermion, with the consequence that no new formulas are needed to implement many-body theory. In conventional electronic many-body theory, one has to take care of two different classes of electrons, associated with α and β spins. Within each class, there are multiple identical fermions, and exchange contributions arise in matrix elements; between each class, exchange integrals are zero. The present formulation is a generalization that introduces additional distinct fermion types. The existing software designed for the electronic problem is easily adapted, with a strong separation of the Hamiltonian representation, and the many-body theory, with the latter being agnostic to the different types of fermions.

Although this formalism is general, and allows a unified treatment of the quantum dynamics of electrons, nuclei, and optical fields, in this paper, we apply it just to the strong coupling of an electronic system with a single optical cavity.

In this case, the reference state is given by the product of an electronic determinant $|\Phi\rangle$ and the photonic vacuum state $|0\rangle$,

$$|\Phi_0\rangle = |\Phi\rangle \otimes |0\rangle, \quad (9)$$

and the excitation operators include both electronic (μ) and photonic (ν) excitations, as well as coupled electron-photon ($\hat{\mu}\hat{\nu}$) terms. Hence, the electron-boson cluster operator has the following form:

$$\hat{\mathcal{T}} = \sum_{\mu} \hat{\tau}_{\mu} + \sum_{\nu} \hat{\tau}_{\nu} + \sum_{\hat{\mu}\hat{\nu}} \hat{\tau}_{\hat{\mu}\hat{\nu}}. \quad (10)$$

Following the nomenclature proposed in Ref. 28, the electronic coupled-cluster single doubles (CCSD) equations correspond to the polaritonic CC-SD-S-D, which includes single and double electronic, single photon, and coupled one-photon one-electron excitations. One should note that in the excitation-operator formalism, the single cavity pseudo-particle excitations include all multiphoton creations up to the size of the cavity one-particle space, i.e., the number of harmonic-oscillator wavefunctions that have been selected as the basis functions.

C. Adiabatic and diabatic approximations

Just as in the electronic case, the first step to solve the total polaritonic Schrödinger equation (SE), which contains the Hamiltonian of Eq. (1), is usually to invoke the Born–Oppenheimer (BO) approximation,³³ also known as the adiabatic approximation. This leads to the polaritonic SE, in which the Hamiltonian does not contain the nuclear kinetic energy (NKE), but depends parametrically on the nuclear coordinates \mathbf{R} ,

$$\hat{\mathcal{H}}_p \Phi_i(\mathbf{r}; \mathbf{R}) = V_i(\mathbf{R}) \Phi_i(\mathbf{r}; \mathbf{R}), \quad (11)$$

and so do its eigenvalues $V_i(\mathbf{R})$ and eigenfunctions $\Phi_i(\mathbf{r}; \mathbf{R})$. The set of eigenfunctions $\{\Phi_i(\mathbf{r}; \mathbf{R})\}$ forms a complete orthonormal basis in the polaritonic space at each value of \mathbf{R} , and they are said to be the adiabatic solutions of the SE.

The solution of the total SE will then be given by the Born–Huang (BH) expansion,³⁴ sometimes also given the name of BO expansion,

$$\Psi(\mathbf{r}; \mathbf{R}) = \sum_i^{N_i} \Phi_i(\mathbf{r}; \mathbf{R}) \chi_i(\mathbf{R}), \quad (12)$$

where the sum runs over all adiabatic solutions and where we have introduced the vibrational expansion coefficients χ_i . If the expansion contains the complete set of adiabatic solutions, it is exact. In practice, however, it needs to be truncated to a computationally feasible number of lowest states.

By inserting the expanded wavefunction of Eq. (12) into the nuclear SE and integrating over electronic coordinates, one arrives at the following expression:³⁵

$$[\hat{T}_n + V_j(\mathbf{R})] \chi_i(\mathbf{R}) - \sum_j \Lambda_{ji} \chi_j(\mathbf{R}) = E \chi_i(\mathbf{R}), \quad (13)$$

which contains the nuclear kinetic energy coupling (NKEC),

$$\Lambda_{ij} = \delta_{ij} T_n - \langle \Phi_i | \hat{T}_n | \Phi_j \rangle. \quad (14)$$

The NKEC describes the dynamical interaction between the polaritonic and nuclear motions and gives rise to the non-adiabatic coupling (NAC). It is inversely proportional to the energy difference between states i and j , thus diverging when the two states become degenerate. In this situation, the BO approximation is known to break down, as the electronic structure quickly changes with small changes in the nuclear geometry, which typically occurs at conical intersections.³⁵

To account for these non-adiabatic effects, it is more convenient to transform the adiabatic basis into one where the NACs are as near to zero as possible, such that they can be neglected, called the diabatic representation.³⁶

This can be achieved by finding a unitary transformation, often given the name of adiabatic-to-diabatic transformation (ADT),

$$\mathbf{W} = \mathbf{U}^\dagger \mathbf{V} \mathbf{U}. \quad (15)$$

In our case, we are interested in the interaction of two polaritonic states; thus, \mathbf{V} refers to the diagonal adiabatic matrix with eigenvalues ε_1 and ε_2 ,

$$\mathbf{V} = \begin{pmatrix} \varepsilon_1 & 0 \\ 0 & \varepsilon_2 \end{pmatrix}, \quad (16)$$

and \mathbf{W} refers to the no-longer diagonal, but symmetric, diabatic matrix,

$$\mathbf{W} = \begin{pmatrix} w_{11} & w_{12} \\ w_{12} & w_{22} \end{pmatrix}. \quad (17)$$

The unitary matrix \mathbf{U} can be taken as the rotation matrix,

$$\mathbf{U} = \begin{pmatrix} \cos \theta & \sin \theta \\ -\sin \theta & \cos \theta \end{pmatrix}, \quad (18)$$

where θ is the mixing angle that gives a measure of the “mixing” between the two polaritonic states. There are different strategies to find the mixing angle; the most rigorous method being to explicitly calculate Λ_{ij} ;^{36–39} however, this is a tedious task and often needs to be approximated.⁴⁰ Therefore, less-demanding methods have been devised, such as property^{41,42} or energy-based methods.^{43–45} Yet a different approach is to obtain it directly by inspection of the wavefunction coefficients,^{40,46,47} which we have employed in this work. The mixing angle can be approximated from the excited-state wavefunctions, as the EOM amplitudes can be expressed as a function of θ ,

$$r_p^{(0) \rightarrow |1\rangle} = \cos \theta, \quad r_e^{(0) \rightarrow |1\rangle} = \sin \theta, \quad (19)$$

where $|0\rangle \rightarrow |1\rangle$ indicates the amplitude corresponding to the occupation of the first photonic state, and p and e indicate that the EOM coefficient corresponds to the wavefunction of the state identified as having stronger photonic ($|\text{GS} + 1p\rangle$) or electronic character ($|\text{ES} + 0p\rangle$), respectively. This is possible as in the special case of a photonic excitation, the excitation is very localized to one single photonic excitation with only negligible contribution of higher-energy photonic states, as opposed as electronic excitations that are usually delocalized over different orbitals. We note here that it is preferable to use the second equation of Eq. (19), since the electronic state mixes with only the lowest photonic state whereas the latter mixes with higher-energy electronic states at larger internuclear distance and is, thus, more error-prone if we want to study its interaction only with the first excited state.

An additional diabaticization strategy has been employed in this study, where the diabatic energies have been calculated directly in the adiabatic basis. This was done by calculating the uncoupled energies (i.e., with the polaritonic coupling turned off) in the basis of the adiabatic coupled solutions. From these diabatic energies, together with the polaritonic eigenvalues ε_1 and ε_2 , one can reconstruct the diabatic matrix from Eq. (17).

Finally, in order to simulate the vibrational spectrum, we need to calculate the relative intensity of each peak, which will be given by the electric transition dipole moment,

$$I^{i,f} \propto |\langle \Psi_f | \hat{\mu} | \Psi_i \rangle|^2. \quad (20)$$

In the adiabatic picture, the transition dipole moment could be calculated by solving the left EOM eigenvalue problem. However, this would increase the computational time by roughly twice the time. Instead, one can simply transform the diabatic transition dipole moments to the adiabatic basis, by using the same adiabatic-to-diabatic transformation as presented above, and by approximating the transition dipole moment by the one obtained from the fully electronic calculation, and assuming that the photonic transition is dark.

III. COMPUTATIONAL DETAILS

The EOM-CC-SD-S-D method presented in Sec. II B has been implemented in a new general many-body `gmb` module by using the `libtensor` library.⁴⁸ It can run as a stand-alone program, or integrated as a part of the `MOLPRO` software package.⁴⁹ The ground-state CC and EOM-CC programmable expressions have the same form as the electronic ones and can, thus, be found elsewhere;^{50,51} whereas the programmable expressions for the polaritonic Hamiltonian are given in Subsection 1 of the Appendix.

The potential energy surfaces have been calculated by using the `gmb` program, which have been subsequently used to compute the vibrational levels by using the `DUO`⁵² program.

The results for the CO molecule presented in Sec. IV have been obtained by using the `cc-pVDZ` basis set,⁵³ with the two lowest σ orbitals omitted from the correlation treatment. The equilibrium geometry has been calculated to be $r_{\text{CO}} = 1.1384 \text{ \AA}$, and all calculations have been run with $n_{\text{max}} = 4$. For the other polaritonic parameters, such as the light–matter coupling strength and the cavity frequency, different values have been taken depending on the calculation and, thus, will be specified when necessary.

IV. RESULTS

We investigate the influence of coupling to cavity modes on the vibrational structure of the electronic absorption spectra. For this purpose, we choose to study the diatomic molecule, carbon monoxide (CO). We will particularly focus on its first bright excited state at the Franck–Condon (FC) geometry, a degenerate Π , and its interaction with the first cavity mode. Adopting the standard orientation, where the CO molecule is along the z axis, we choose the cavity polarization direction to be x . This will cause a breakdown of degeneracy of the Π_x and Π_y states due to the coupling between the π_x and the first photonic states.

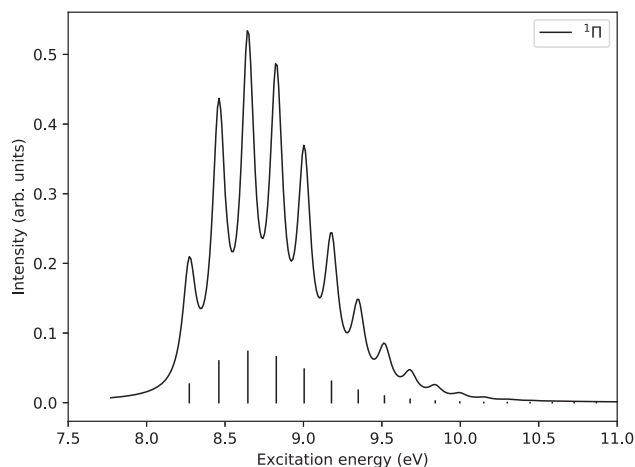


FIG. 3. Vibrational absorption spectrum of the $A^1\Pi$ state of CO, calculated in the absence of coupling to the cavity.

Figure 3 corresponds to the vibrationally resolved absorption spectrum arising from the ground state in the absence of any cavity, and shows the usual progression in the vibrational states of the $A^1\Pi$ state.

To form a polariton, the cavity frequency needs to be in resonance with the electronic state excitation energy, such that photonic and electronic states can interact with each other. Thus, we set the cavity frequency to 0.32 Ha to 8.7 eV and start by studying the effects of changing the coupling strength γ .

We start by considering the BO approximation; in the adiabatic picture, the LP and the UP states form an avoided crossing where they switch character. The PESs are shown in Fig. 4 for the cavity frequency $\omega_c = 8.7$ eV and different values for the coupling strength. The PESs show the same trend as previous studies,^{28,29} One can see that the two states cross for $\gamma = 0$ around the equilibrium geometry; however, once the coupling is switched on, they move away from each other. As expected, the larger the coupling strength, the farther

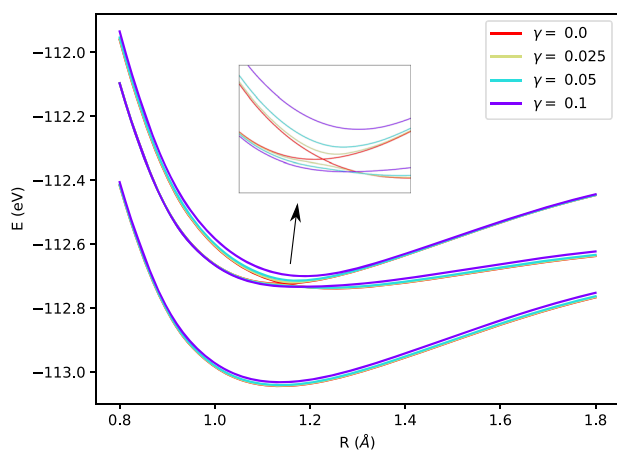


FIG. 4. Adiabatic PESs for CO using $\omega_c = 8.7$ eV and for different values of γ .

apart are the two states at the crossing bond length; with $\gamma = 0.1$, the minimum separation of the polaritonic potential energy curves is 0.90 eV and the equilibrium-to-equilibrium excitation energy to the first excited state is 8.16 eV, 0.64 eV below that of the pure electronic problem. At larger internuclear distances, one can see how the energy is blue-shifted for the ground state and the first excited states, which corresponds to the self-energy term of the QED Hamiltonian. The fact that the UP state does not show this shift is probably due to the fact that it couples to higher-energy states, thus, lowering its total energy and compensating for the self-energy term.

The vibrational spectra for these curves are shown in Fig. 5. The strongly perturbed energy curves already anticipated that the changes in the spectra would be significant. This is now confirmed in

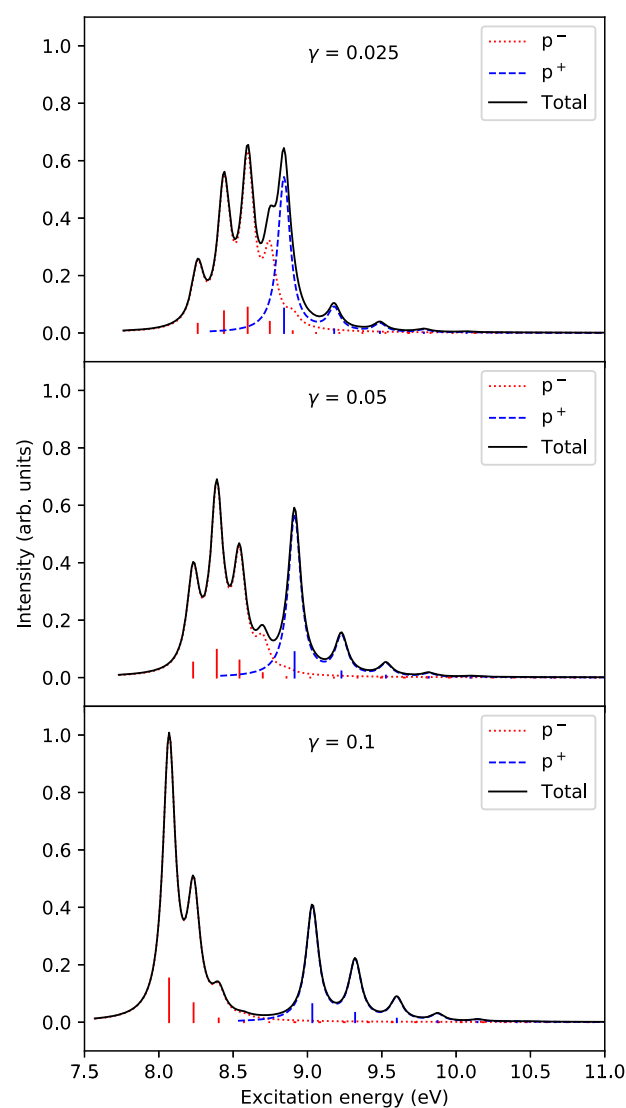


FIG. 5. Vibrationally resolved spectra for CO using $\omega_c = 8.7$ eV and for different values of γ , using the adiabatic states.

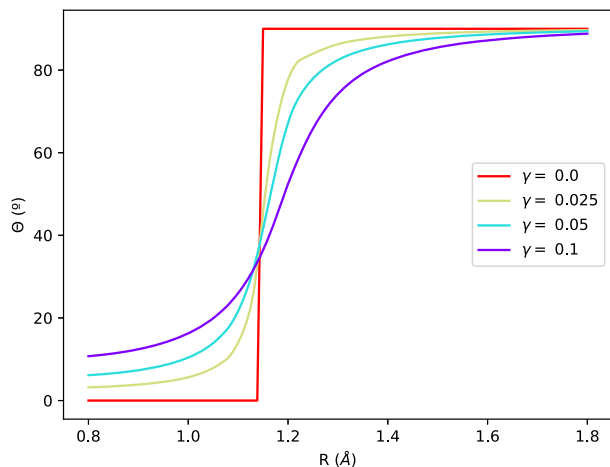


FIG. 6. CO mixing angle (θ , $^\circ$) as a function of the internuclear distance (R , \AA) calculated from the wavefunction coefficients.

Fig. 5, which shows two distinct states with different vibrational progression, both corresponding to a mix of the ground-state and the first excited-state vibrational structure. The low-energy region of the spectrum is strongly red-shifted (by ~ 0.2 eV for $\gamma = 0.1$). Two main trends can be drawn from these spectra. The first is that one can see that the larger the coupling, the larger is the separation between the two first intense peaks, in agreement to the energy separation already seen in the PES. The second refers to the difference in the relative intensity between the two mixed states, as the LP seems to gain intensity when the coupling increases to the detriment of intensity of the UP state.

To check the validity of the adiabatic approximation, we need to assess the importance of the NAC. Thus, we proceed as described in Sec. II C.

Figure 6 shows the mixing angle θ as a function of the internuclear distance for the different values of γ considered, calculated

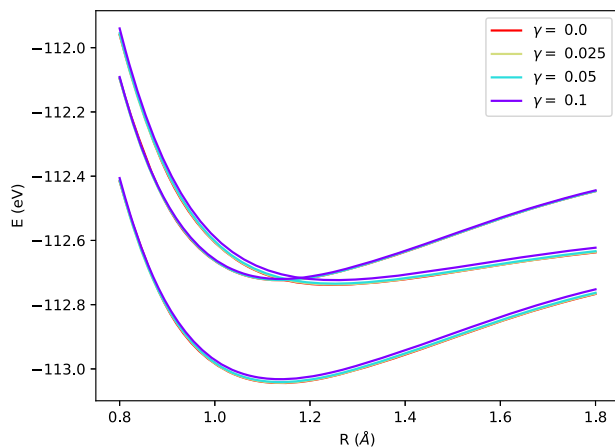


FIG. 7. Diabatic energy curves for CO using $\omega_c = 8.7$ eV and for different values of γ .

from the wavefunction coefficients. One can see that for a zero coupling, this corresponds to a step function, where the mixing angle is 0° before the crossing and 90° after a sudden change, testifying that there is no mixing between the two states. When increasing the coupling strength, the mixing becomes apparent already at $R = 0.8$ \AA and the change of character from one state to the other is more smooth, asymptotically approaching 90° for large values of R . The diabaticized energy curves calculated with this strategy are shown in Fig. 7. The two curves now cross for any value of coupling strength and the different profiles are rather similar, showing only slight differences in energy. These coupled curves give rise to the new spectra, visible in Fig. 8, where the following notation has been introduced: ψ_{n_e, n_λ} with n_e and n_λ indicating the diabatic

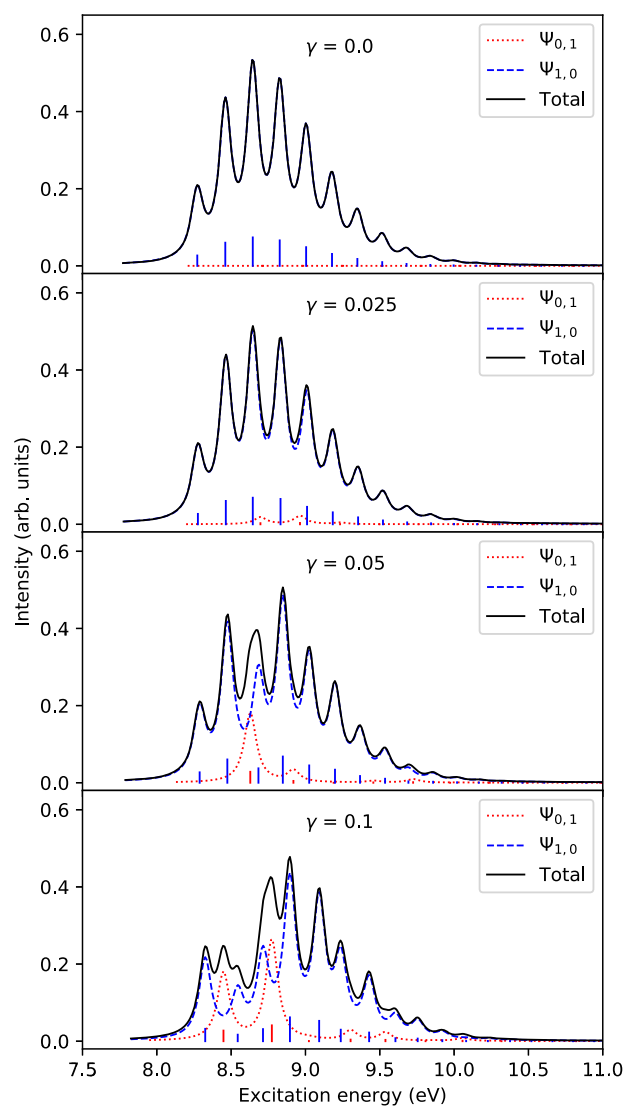


FIG. 8. Vibrationally resolved spectra for CO using $\omega_c = 8.7$ eV and for different values of γ , using the diabatic states calculated from the wavefunction coefficients.

electronic and photonic states respectively. One can clearly recognize the spectrum for $\gamma = 0.0$, which overlaps perfectly with the purely electronic spectrum in Fig. 3. This is only slightly perturbed when setting $\gamma = 0.025$; this change is minimal and can barely be appreciated. However, a substantial change can be observed when using a stronger coupling; for $\gamma = 0.05$, one can already notice a change in the peak intensities. When looking at the spectrum corresponding to the largest coupling strength, the vibrational structure is though completely disturbed.

The stronger changes are led by the $\Psi_{0,1}$ state, where two main effects can be observed. The first is an increase in its intensity, due to a higher intensity borrowing induced by a stronger coupling. The second is that the low-energy spectrum is red-shifted, and the higher-frequency vibronic absorptions are blue-shifted. This effect is consistent with a first-order perturbation theory interpretation, where vibronic states of Σ^+ , Π symmetries are coupled by the part of the polaritonic Hamiltonian that is linear in γ , which causes in the usual way the eigenvalue spectrum to be widened but the average of all eigenvalues to be conserved. Higher-order effects, and the difference of self-energy between the ground and excited states, introduce further shifts in the spectrum.

The strong polaritonic mixing means that the electron-plus-cavity wavefunction changes strongly with geometry, and the effects of the nuclear kinetic energy operator on it cannot be neglected. When the polaritonic coupling is introduced in the diabatic basis, the strong red-shift of the spectrum that arises in the BO calculation from the polaritonic interaction, pushing the potential energy function to lower energy, does not arise to the same extent. This implies that merely observing the effect of polaritonic coupling on potential energy surfaces is not a sufficient route to understanding physically observable quantities.

To check the validity of the wavefunction diabaticization scheme, we now attempt to reproduce its results by employing the other diabaticization method described in Sec. II C, that is, by computing directly the diabatic energies in the adiabatic basis. The spectrum obtained by using this procedure can be found in Fig. 9. Comparing it to the bottom spectrum of Fig. 8, a noticeable difference can be appreciated when looking at the contribution of each of the two states to the total spectrum. This is particularly true for the state assigned as $\psi_{0,1}$. However, the overall trend of the total spectra is similar for both schemes.

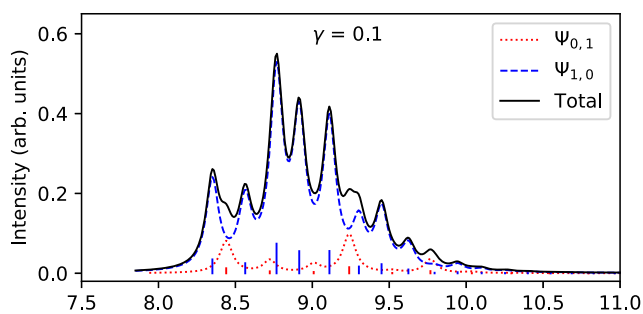


FIG. 9. Vibrationally resolved spectra for CO using $\omega_c = 8.7$ eV and $\gamma = 0.1$, using the diabatic states calculated in the adiabatic basis.

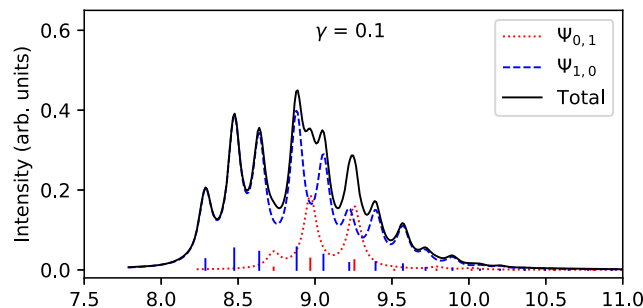


FIG. 10. Vibrationally resolved spectra for CO using $\omega_c = 8.7$ eV and $\gamma = 0.1$, using the diabatic states calculated without polaritonic coupling.

As a third diabatic scheme, we consider now using as diabatic states the uncoupled states ($|\text{GS} + 1p\rangle$ and $|\text{ES} + 0p\rangle$) calculated including the self-energy contribution, whereas the polaritonic coupling is only introduced perturbatively afterward. These results are shown in Fig. 10. The total spectrum shows some similarities with the ones in Figs. 8 (bottom) and 9; however, the individual contributions of each state to the spectrum are substantially different. In particular, the spectral signature of $\Psi_{0,1}$ is blue-shifted with respect to the previous results. Thus, this shift alters mainly the higher-energy region of the total spectrum as opposed as Fig. 8, where the vibrational progression was mainly affected at the lower-energy region. This blue shift with respect to the polaritonic calculation of Fig. 8 can be attributed to the omission of electron-cavity dynamic correlation in this approach, which would appear in the wavefunction as entanglement of many excited electronic states with various cavity modes. Thus, this result shows that a fully polaritonic calculation is needed to ensure a correct description of the vibronic spectra of polaritonic systems. Because none of the diabaticization schemes are perfect, we attempted to devise other perturbative schemes to further assess these results. However, for some geometries, the difference in energy

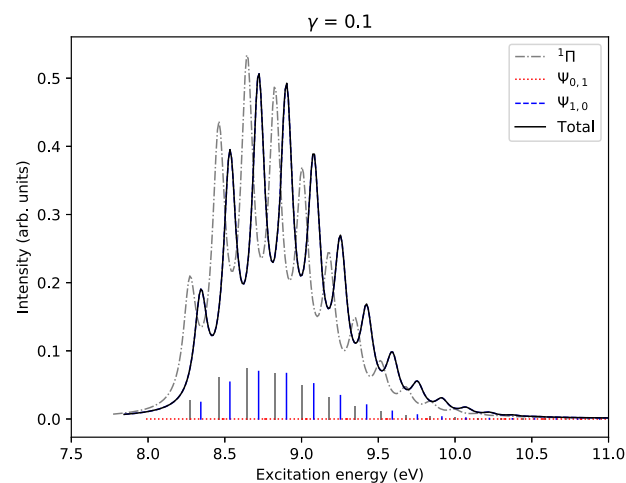


FIG. 11. Vibrationally resolved spectra for CO using $\gamma = 0.1$ with coupling turned off, compared to the fully electronic $A^1\Pi$ state spectrum.

between the diabatic states obtained was inferior to the coupling value, yielding imaginary energies. These schemes were, therefore, discarded.

Nonetheless, we do believe that the results obtained from the mixing angle give a good idea of how the CO spectrum for the $A^1\Pi$ state would look like when coupled to an optical cavity mode. This is supported by the results obtained using the other diabaticization schemes.

To assess the importance of the polaritonic coupling, we show, in Fig. 11, the spectrum obtained when switching it off. This figure shows that, in the absence of coupling between the two diabatic curves, the obtained spectrum is very similar to the one obtained in

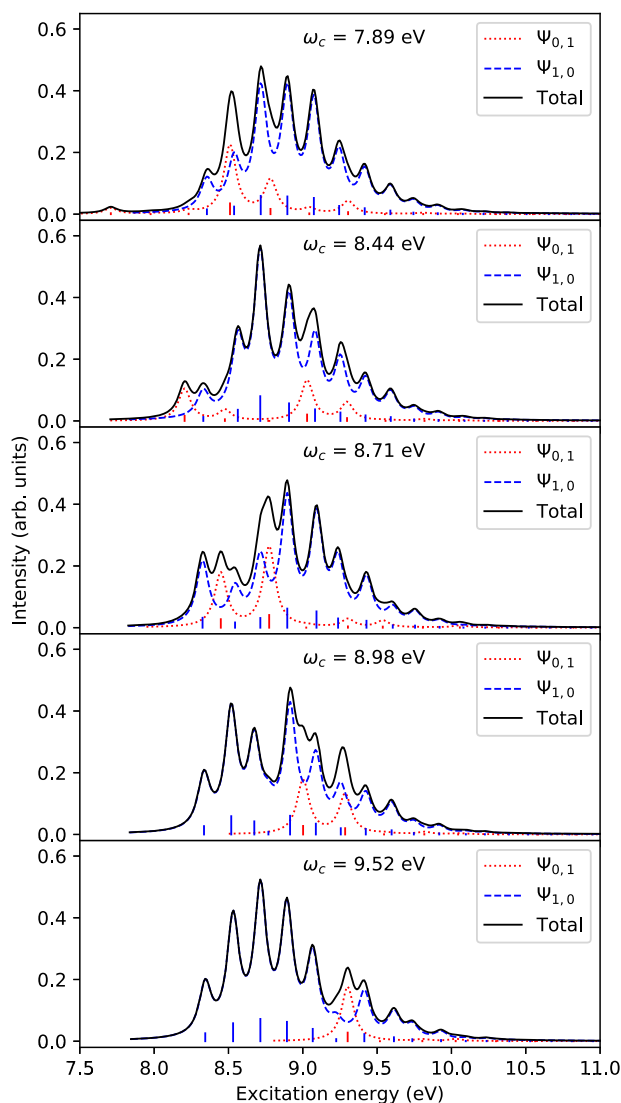


FIG. 12. Vibrationally resolved spectra for CO using $\gamma = 0.1$ and for different values of ω_c , using the diabatic states calculated from the wavefunction coefficients.

the absence of any cavity; the main difference being a slight blue-shift in the energy, which can be rationalized by the self-energy term.

After investigating the effects of tuning the coupling strength on the vibrational spectrum, we turn now our attention to exploring the changes induced when modifying instead the cavity frequency by scanning the region where both states are in resonance ($\omega_c = 7.9$ – 9.5 eV) for a fixed coupling strength ($\gamma = 0.1$). These results are presented in Fig. 12, where the spectra have been obtained from the wavefunction coefficients of the diabaticization scheme. These are in agreement with what one could expect; at the lower and upper ends, the presence of a cavity only minimally affects the original electronic spectrum at the respective ends. This is primarily due to the fact that the energy needed to populate the photonic state corresponds to the edges of the spectrum, and also because of this mismatch in energy between the two states, the coupling is weaker and, thus, is the intensity of the $\psi_{0,1}$ state. In contrast, when the cavity frequency starts to approach the electronic excitation energy (~ 8.8 eV), the spectrum is considerably altered. In the same manner, this is both a result of the fact that now the spectra for the two coupled states overlap and that the intensity “borrowed” by the $\psi_{0,1}$ state is now larger as the coupling is stronger. Therefore, this figure illustrates how tuning the cavity frequency alters the spectral signature, testifying to how the presence of an optical cavity can modify the properties of an electronic system.

V. CONCLUSIONS

We have presented a new computational framework for treating polaritonic systems, which has been implemented in the `gmb` program. We have studied how the polaritonic effects alter the vibrational structure of the first electronic state of the CO molecule, in resonance with the cavity mode. To get a complete picture of the different effects that play a role in the vibronic spectrum, we have studied different cases. In the first part, we have simulated the spectra within the Born–Oppenheimer approximation. In this adiabatic picture, the interaction between photons and electrons gives rise to two different states—a lower polariton and an upper polariton—with mixed character. Each state has its particular vibrational structure, which gets farther apart when increasing the coupling strength. In the second part, we have studied how the diabatic picture changes the spectra by allowing the two states to couple. To do so, we have devised two different diabaticization schemes that account for the non-adiabatic effects—one that exploits the EOM wavefunction coefficients and the other that needs the calculation of the diabatic energies in the adiabatic basis. The results show that the BO approximation is not good enough to treat these systems, but a coupled treatment needs to be used in order to reproduce the spectrum. As a third diabatic picture, we also considered directly taking the uncoupled states ($|GS + 1p\rangle$ and $|ES + 0p\rangle$) and introducing the polaritonic coupling perturbatively. However, this approach cannot account for the dynamic correlation, which turned out to be necessary for an accurate simulation of polaritonic systems, and testifying, thus, to the necessity of a fully polaritonic description.

Furthermore, we have shown that the interaction with photons changes considerably the vibrational structure of the electronic

states, and can thus be used to probe the presence of polaritonic states.

The work presented herein has been implemented in a general and modular manner paving the way for future work where the interacting particles do not need to be restrained to electrons and photons. In a future study, we intend to use the same framework to address the coupling between vibrations and electrons.

ACKNOWLEDGMENTS

The authors acknowledge funding from the EPSRC (Grant Nos. EP/R014493/1 and EP/R014183/1). The authors also acknowledge the support of the Supercomputing Wales project, which is partly funded by the European Regional Development Fund (ERDF) via Welsh Government. The authors thank Evgeny Epifanovsky for helpful discussions about `libtensor`. The authors also thank Jonathan Tennyson and Qianwei Qu for helpful discussions about `DUO`.

AUTHOR DECLARATIONS

Conflict of Interest

The authors have no conflicts to disclose.

DATA AVAILABILITY

The data that support the findings of this study are available from the corresponding author upon reasonable request.

APPENDIX: PROGRAMMABLE EXPRESSIONS

1. Polaritonic Hamiltonian

The polaritonic Hamiltonian can be written in atomic units,

$$\hat{\mathcal{H}} = \hat{\mathcal{H}}_e + \sum_{\kappa} \left(\omega_{\kappa} \hat{b}_{\kappa}^{\dagger} \hat{b}_{\kappa} - \gamma_{\kappa} \omega_{\kappa} \hat{\mu} \left(\hat{b}_{\kappa}^{\dagger} + \hat{b}_{\kappa} \right) + \gamma_{\kappa}^2 \omega_{\kappa} \hat{\mu}^2 \right), \quad (\text{A1})$$

where the photonic part has been taken as the shifted harmonic oscillator. To ensure origin-independence, $\hat{\mu}$ refers to the total dipole operator, including both nuclear and electronic contributions: $\hat{\mu} = \hat{\mu}_N + \hat{\mu}_e$. Thus, it can be rewritten as

$$\hat{\mathcal{H}} = \hat{\mathcal{H}}_e + \sum_{\kappa} \left(\omega_{\kappa} \hat{b}_{\kappa}^{\dagger} \hat{b}_{\kappa} - \gamma_{\kappa} \omega_{\kappa} \hat{\mu}_N \left(\hat{b}_{\kappa}^{\dagger} + \hat{b}_{\kappa} \right) - \gamma_{\kappa} \omega_{\kappa} \hat{\mu}_e \left(\hat{b}_{\kappa}^{\dagger} + \hat{b}_{\kappa} \right) + \gamma_{\kappa}^2 \omega_{\kappa} \hat{\mu}_N^2 + 2\gamma_{\kappa}^2 \omega_{\kappa} \hat{\mu}_N \hat{\mu}_e + \gamma_{\kappa}^2 \omega_{\kappa} \hat{\mu}_e^2 \right). \quad (\text{A2})$$

Consider the second-quantized Hamiltonian,

$$\hat{H} = \hat{V} + \sum_{\sigma} \hat{a}_{\sigma v}^{\dagger} \hat{a}_{\sigma w} h_{vw}^{\sigma} + \frac{1}{4} \sum_{\tau\sigma} \hat{a}_{\sigma v}^{\dagger} \hat{a}_{\tau x}^{\dagger} \hat{a}_{\tau y} \hat{a}_{\sigma w} \langle vx || wy \rangle^{\sigma\tau}, \quad (\text{A3})$$

where σ and τ range over the particle types:

- α and β : Electrons with a particular spin.
- κ, λ, \dots : Optical cavity modes.

Assuming the same spatial parts for α - and β -spin electronic basis functions, we can identify the different contributions as follows:

- Scalar part:

$$\hat{V} = \hat{V}_{NN} + \sum_{\kappa} \gamma_{\kappa}^2 \omega_{\kappa} \hat{\mu}_N^2. \quad (\text{A4})$$

- One-particle part:

- One-electron:

$$h_{pq}^{\alpha} = h_{pq}^e + \sum_{\kappa} \left(\gamma_{\kappa}^2 \omega_{\kappa} \mu_{pq}^2 + 2\gamma_{\kappa}^2 \omega_{\kappa} \mu_{N} \mu_{pq} \right), \quad (\text{A5})$$

where h_{pq}^e is the usual one-electron Hamiltonian,

$$h_{pq}^e = \langle p | -\frac{1}{2} \nabla^2 + \hat{V}_{eN} | q \rangle. \quad (\text{A6})$$

- One-photon:

$$h_{pq}^{\kappa} = p \omega_{\kappa} \delta_{pq} - \gamma_{\kappa} \omega_{\kappa} \hat{\mu}_N \times \left(\sqrt{q+1} \delta_{p,q+1} + \sqrt{q} \delta_{p,q-1} \right). \quad (\text{A7})$$

- Two-particle part:

- Two-photon:

$$\langle pr || qs \rangle^{\sigma\tau} = (pq || rs) - \delta_{\sigma\tau} (ps || rq) + \sum_{\kappa} 2\gamma_{\kappa}^2 \omega_{\kappa} (\mu_{pr} \mu_{qs} - \delta_{\sigma\tau} \mu_{qr} \mu_{ps}). \quad (\text{A8})$$

- Two-electron:

$$\langle pr || qs \rangle^{\kappa\lambda} = 0. \quad (\text{A9})$$

- Electron-photon:

$$\langle pr || qs \rangle^{\sigma\kappa} = -\gamma_{\kappa} \omega_{\kappa} \mu_{pq} \left(\sqrt{s+1} \delta_{r,s+1} + \sqrt{s} \delta_{r,s-1} \right). \quad (\text{A10})$$

REFERENCES

- ¹Y. Kaluzny, P. Goy, M. Gross, J. M. Raimond, and S. Haroche, "Observation of self-induced Rabi oscillations in two-level atoms excited inside a resonant cavity: The ringing regime of superradiance," *Phys. Rev. Lett.* **51**, 1175–1178 (1983).
- ²P. G. Savvidis, J. J. Baumberg, R. M. Stevenson, M. S. Skolnick, D. M. Whittaker, and J. S. Roberts, "Angle-resonant stimulated polariton amplifier," *Phys. Rev. Lett.* **84**, 1547–1550 (2000).
- ³Y. Yamamoto, "Half-matter, half-light amplifier," *Nature* **405**, 629–630 (2000).
- ⁴T. H. Stievater, X. Li, D. G. Steel, D. Gammon, D. S. Katzer, D. Park, C. Piermarocchi, and L. J. Sham, "Rabi oscillations of excitons in single quantum dots," *Phys. Rev. Lett.* **87**, 133603 (2001).
- ⁵J. M. Raimond, M. Brune, and S. Haroche, "Manipulating quantum entanglement with atoms and photons in a cavity," *Rev. Mod. Phys.* **73**, 565–582 (2001).
- ⁶T. Schwartz, J. A. Hutchison, C. Genet, and T. W. Ebbesen, "Reversible switching of ultrastrong light-molecule coupling," *Phys. Rev. Lett.* **106**, 196405 (2011).
- ⁷J. Yuen-Zhou, W. Xiong, and T. Shegai, "Polariton chemistry: Molecules in cavities and plasmonic media," *J. Chem. Phys.* **156**, 030401 (2022).

- ⁸T. W. Ebbesen, “Hybrid light–matter states in a molecular and material science perspective,” *Acc. Chem. Res.* **49**, 2403–2412 (2016).
- ⁹K. Stranius, M. Hertzog, and K. Börjesson, “Selective manipulation of electronically excited states through strong light–matter interactions,” *Nat. Commun.* **9**, 2273 (2018).
- ¹⁰B. Munkhbat, M. Wersäll, D. G. Baranov, T. J. Antosiewicz, and T. Shegai, “Suppression of photo-oxidation of organic chromophores by strong coupling to plasmonic nanoantennas,” *Sci. Adv.* **4**, eaas9552 (2018).
- ¹¹J. A. Hutchison, T. Schwartz, C. Genet, E. Devaux, and T. W. Ebbesen, “Modifying chemical landscapes by coupling to vacuum fields,” *Angew. Chem., Int. Ed.* **51**, 1592–1596 (2012).
- ¹²A. Thomas, J. George, A. Shalabney, M. Dryzhakov, S. J. Varma, J. Moran, T. Chervy, X. Zhong, E. Devaux, C. Genet, J. A. Hutchison, and T. W. Ebbesen, “Ground-state chemical reactivity under vibrational coupling to the vacuum electromagnetic field,” *Angew. Chem., Int. Ed.* **55**, 11462–11466 (2016).
- ¹³J. Lather, P. Bhatt, A. Thomas, T. W. Ebbesen, and J. George, “Cavity catalysis by cooperative vibrational strong coupling of reactant and solvent molecules,” *Angew. Chem., Int. Ed.* **58**, 10635–10638 (2019).
- ¹⁴A. Thomas, L. Lethuillier-Karl, K. Nagarajan, R. M. A. Vergauwe, J. George, T. Chervy, A. Shalabney, E. Devaux, C. Genet, J. Moran, and T. W. Ebbesen, “Tilting a ground-state reactivity landscape by vibrational strong coupling,” *Science* **363**, 615–619 (2019).
- ¹⁵E. Orgiu, J. George, J. A. Hutchison, E. Devaux, J. F. Dayen, B. Doudin, F. Stellacci, C. Genet, J. Schachenmayer, C. Genes, G. Pupillo, P. Samori, and T. W. Ebbesen, “Conductivity in organic semiconductors hybridized with the vacuum field,” *Nat. Mater.* **14**, 1123–1129 (2015).
- ¹⁶B. S. Simpkins, K. P. Fears, W. J. Dressick, B. T. Spann, A. D. Dunkelberger, and J. C. Owrutsky, “Spanning strong to weak normal mode coupling between vibrational and Fabry–Pérot cavity modes through tuning of vibrational absorption strength,” *ACS Photonics* **2**, 1460–1467 (2015).
- ¹⁷F. J. Garcia-Vidal, C. Ciuti, and T. W. Ebbesen, “Manipulating matter by strong coupling to vacuum fields,” *Science* **373**, eabd0336 (2021).
- ¹⁸F. S. Bergeret and I. V. Tokatly, “Single-triplet conversion and the long-range proximity effect in superconductor-ferromagnet structures with generic spin dependent fields,” *Phys. Rev. Lett.* **110**, 117003 (2013).
- ¹⁹M. Ruggenthaler, J. Flick, C. Pellegrini, H. Appel, I. V. Tokatly, and A. Rubio, “Quantum-electrodynamical density-functional theory: Bridging quantum optics and electronic-structure theory,” *Phys. Rev. A* **90**, 012508 (2014).
- ²⁰J. Flick, M. Ruggenthaler, H. Appel, and A. Rubio, “Kohn–Sham approach to quantum electrodynamic density-functional theory: Exact time-dependent effective potentials in real space,” *Proc. Natl. Acad. Sci. U. S. A.* **112**, 15285–15290 (2015).
- ²¹F. Coester, “Bound states of a many-particle system,” *Nucl. Phys.* **7**, 421–424 (1958).
- ²²F. Coester and H. Kümmel, “Short-range correlations in nuclear wave functions,” *Nucl. Phys.* **17**, 477–485 (1960).
- ²³J. Čížek, “On the correlation problem in atomic and molecular systems. Calculation of wavefunction components in Ursell-type expansion using quantum-field theoretical methods,” *J. Chem. Phys.* **45**, 4256–4266 (1966).
- ²⁴J. Čížek, “On the use of the cluster expansion and the technique of diagrams in calculations of correlation effects in atoms and molecules,” *Adv. Chem. Phys.* **14**, 35–89 (1969).
- ²⁵J. Čížek and J. Paldus, “Correlation problems in atomic and molecular systems III. Rederivation of the coupled-pair many-electron theory using the traditional quantum chemical methods,” *Int. J. Quantum Chem.* **5**, 359–379 (1971).
- ²⁶O. Christiansen, “Vibrational coupled cluster theory,” *J. Chem. Phys.* **120**, 2149–2159 (2004).
- ²⁷O. Christiansen, “A second quantization formulation of multimode dynamics,” *J. Chem. Phys.* **120**, 2140–2148 (2004).
- ²⁸U. Mordovina, C. Bungey, H. Appel, P. J. Knowles, A. Rubio, and F. R. Manby, “Polaritonic coupled-cluster theory,” *Phys. Rev. Res.* **2**, 023262 (2020).
- ²⁹T. S. Haugland, E. Ronca, E. F. Kjønstad, A. Rubio, and H. Koch, “Coupled cluster theory for molecular polaritons: Changing ground and excited states,” *Phys. Rev. X* **10**, 041043 (2020).
- ³⁰T. S. Haugland, C. Schäfer, E. Ronca, A. Rubio, and H. Koch, “Intermolecular interactions in optical cavities: An *ab initio* QED study,” *J. Chem. Phys.* **154**, 094113 (2021).
- ³¹A. E. DePrince, “Cavity-modulated ionization potentials and electron affinities from quantum electrodynamics coupled-cluster theory,” *J. Chem. Phys.* **154**, 094112 (2021).
- ³²J. F. Stanton and R. J. Bartlett, “The equation of motion coupled-cluster method. A systematic biorthogonal approach to molecular excitation energies, transition probabilities, and excited state properties,” *J. Chem. Phys.* **98**, 7029–7039 (1993).
- ³³M. Born and R. Oppenheimer, “Zur quantentheorie der molekeln,” *Ann. Phys.* **389**, 457–484 (1927).
- ³⁴M. Born and K. Huang, *Dynamical Theory of Crystal Lattices* (Oxford University Press, 1956).
- ³⁵W. Domcke, D. Yarkony, and H. Köppel, *Conical Intersections: Electronic Structure, Dynamics & Spectroscopy* (World Scientific, 2004), Vol. 15.
- ³⁶F. T. Smith, “Diabatic and adiabatic representations for atomic collision problems,” *Phys. Rev.* **179**, 111–123 (1969).
- ³⁷M. Baer, “Adiabatic and diabatic representations for atom-molecule collisions: Treatment of the collinear arrangement,” *Chem. Phys. Lett.* **35**, 112–118 (1975).
- ³⁸Z. H. Top and M. Baer, “Incorporation of electronically nonadiabatic effects into bimolecular reactive systems. I. Theory,” *J. Chem. Phys.* **66**, 1363–1371 (1977).
- ³⁹M. Baer, “Electronic non-adiabatic transitions derivation of the general adiabatic-diabatic transformation matrix,” *Mol. Phys.* **40**, 1011–1013 (1980).
- ⁴⁰A. J. Dobbyn and P. J. Knowles, “A comparative study of methods for describing non-adiabatic coupling: Diabatic representation of the $^1\Sigma^+ / ^1\Pi$ HOH and HHO conical intersections,” *Mol. Phys.* **91**, 1107–1124 (1997).
- ⁴¹A. Macias and A. Riera, “Calculation of diabatic states from molecular properties,” *J. Phys. B: At. Mol. Phys.* **11**, L489–L492 (1978).
- ⁴²H.-J. Werner and W. Meyer, “MCSCF study of the avoided curve crossing of the two lowest $^1\Sigma^+$ states of LiF,” *J. Chem. Phys.* **74**, 5802–5807 (1981).
- ⁴³C. Woywod, W. Domcke, A. L. Sobolewski, and H.-J. Werner, “Characterization of the S_1 – S_2 conical intersection in pyrazine using *ab initio* multiconfiguration self-consistent-field and multireference configuration-interaction methods,” *J. Chem. Phys.* **100**, 1400–1413 (1994).
- ⁴⁴A. Thiel and H. Köppel, “Proposal and numerical test of a simple diabaticization scheme,” *J. Chem. Phys.* **110**, 9371–9383 (1999).
- ⁴⁵H. Köppel, J. Gronki, and S. Mahapatra, “Construction scheme for regularized diabatic states,” *J. Chem. Phys.* **115**, 2377–2388 (2001).
- ⁴⁶H. J. Werner, B. Follmeg, and M. H. Alexander, “Adiabatic and diabatic potential energy surfaces for collisions of $CN(X^2\Sigma^+, A^2\Pi)$ with He,” *J. Chem. Phys.* **89**, 3139–3151 (1988).
- ⁴⁷B. Heumann, K. Weide, R. Dören, and R. Schinke, “Nonadiabatic effects in the photodissociation of H_2S in the first absorption band: An *ab initio* study,” *J. Chem. Phys.* **98**, 5508–5525 (1993).
- ⁴⁸E. Epifanovsky, M. Wormit, T. Kuś, A. Landau, D. Zuev, K. Khistyayev, P. Manohar, I. Kaliman, A. Dreuw, and A. I. Krylov, “New implementation of high-level correlated methods using a general block tensor library for high-performance electronic structure calculations,” *J. Comput. Chem.* **34**, 2293–2309 (2013).
- ⁴⁹H.-J. Werner, P. J. Knowles, F. R. Manby, J. A. Black, K. Doll, A. Heßelmann, D. Kats, A. Köhn, T. Korona, D. A. Kreplin, Q. Ma, T. F. Miller, A. Mitrushchenkov, K. A. Peterson, I. Polyak, G. Rauhut, and M. Sibaev, “The Molpro quantum chemistry package,” *J. Chem. Phys.* **152**, 144107 (2020).
- ⁵⁰T. D. Crawford and H. F. Schaefer III, “An introduction to coupled cluster theory for computational chemists,” *Rev. Comput. Chem.* **14**, 33–136 (2000).
- ⁵¹I. Shavitt and R. J. Bartlett, *Many-Body Methods in Chemistry and Physics* (Cambridge University Press, 2009).
- ⁵²S. N. Yurchenko, L. Lodi, J. Tennyson, and A. V. Stolyarov, “DUO: A general program for calculating spectra of diatomic molecules,” *Comput. Phys. Commun.* **202**, 262–275 (2016).
- ⁵³T. H. Dunning, “Gaussian basis sets for use in correlated molecular calculations. I. The atoms boron through neon and hydrogen,” *J. Chem. Phys.* **90**, 1007–1023 (1989).